Generalized Multiscale Discontinuous Galerkin Method for Helmholtz Problem in Fractured Media

U. Gavrileva[1(✉)], V. Alekseev[1], M. Vasilyeva[1,2], J. D. De Basabe[3], Y. Efendiev[4], and R. L. Gibson Jr.[5]

[1] Multiscale Model Reduction Laboratory, North-Eastern Federal University, Yakutsk, Russia
lanasemna@mail.ru
[2] Institute for Scientific Computation, Texas A&M University, College Station, TX, USA
vasilyevadotmdotv@gmail.com
[3] Department of Seismology, Earth Sciences Division, CICESE, Baja California, Mexico
[4] Department of Mathematics and Institute for Scientific Computation (ISC), Texas A&M University, College Station, TX, USA
[5] Department of Geology and Geophysics, Texas A&M University, College Station, TX, USA

Abstract. In this work, we consider wave propagation in fractured media. The mathematical model is described by Helmholtz problem related to wave propagation with specific interface conditions on the fracture in the frequency domain. We use a discontinuous Galerkin method for the approximation by space that help to weakly impose interface conditions on fractures. Such approximations lead to the large system of equations and computationally expensive. In this work, we construct a coarse grid approximation for effective solution using Generalized Multiscale Discontinuous Galerkin Method (GMsDGM). In this method, we construct a multiscale space using solution of the local spectral problems in each coarse elements. The results of the numerical solution for the two-dimensional problem are presented for model problems of the wave propagation in fractured media.

Keywords: Fractured media · Wave propagation · Helmholtz equation · Discontinuous Galerkin method · Multiscale method · GMsFEM

1 Problem Formulation

We consider the Helmholtz equation for the elastic waves propagation in the computational domain Ω [1,2]

$$-\operatorname{div}\sigma - \omega^2 \rho u = f, \quad x \in \Omega \tag{1.1}$$

I. Dimov et al. (Eds.): FDM 2018, LNCS 11386, pp. 250–257, 2019.
https://doi.org/10.1007/978-3-030-11539-5_27

where ω is frequency, ρ is density and f is the source function.

Equation (1.1) is supplemented by the relation between the stress tensor σ and strain tensor ε

$$\varepsilon(u) = \frac{1}{2}(\nabla u + (\nabla u)^T), \quad \sigma(u) = 2\mu\varepsilon(u) + \lambda \operatorname{div} u\, E \tag{1.2}$$

where E is unit tensor, λ and μ are Lame parameters.

The problem is considered in fractured media. For numerical simulations of the elastic wave equation in the fractured media, we apply the linear-slip model (LSM) [3,4]. Specifically, we assume that the fractures have a vanishing width across which the tractions are taken to be continuous. Following the linear-slip model, we have a linear relation between traction vector and the magnitude of the discontinuity in the displacement field as follows

$$[u] = Z\sigma \cdot n, \tag{1.3}$$

where $[u]$ is the jump of the displacement field at the fracture, $\sigma \cdot n$ is the traction vector at the surface of the fracture and Z is the fracture compliance matrix.

The compliance matrix is characterized in terms of two parameters. For the fracture with up-down symmetry and rotational symmetry about the normal, the fracture compliance matrix is diagonal

$$Z = \begin{bmatrix} z_1 & 0 \\ 0 & z_2 \end{bmatrix}$$

where $z_1 = k_1^{-1}$ and $z_2 = k_2^{-1}$ are the normal and tangential compliances, respectively.

In the computations, the energy of waves needs to be absorbed in artificial boundaries in order to avoid spurious reflections caused by the finite computational domain [5]. We use a first order absorbing boundary condition

$$i\rho\omega Au = -\sigma(u)n, \quad x \in \partial\Omega, \tag{1.4}$$

where

$$A = \begin{bmatrix} n_1 & n_2 \\ -n_2 & n_1 \end{bmatrix} \begin{bmatrix} c_p & 0 \\ 0 & c_s \end{bmatrix} \begin{bmatrix} n_1 & -n_2 \\ n_2 & n_1 \end{bmatrix}.$$

Here $n = (n_1, n_2)$ is the outward normal to the boundary and

$$c_p = \sqrt{\frac{\lambda + 2\mu}{\rho}}, \quad c_s = \sqrt{\frac{\mu}{\rho}} \tag{1.5}$$

where c_s, c_p are the S- and P-wave velocities.

2 Fine Grid Approximation

For the fine-grid approximation, we use the Interior Penalty Discontinuous Galerkin (IPDG) finite element method that allows for discontinuities in the

displacement field to simulate fractures with the linear-slip model [6–8]. Let E be the edge between the elements K_1 and K_2, then the average and jump of a vector function u on E are given by

$$\{u\} = \frac{u\mid_{K_1} + u\mid_{K_2}}{2}, \quad [u] = u\mid_{K_1} - u\mid_{K_2}.$$

Let $\mathcal{T}_h$ denote a finite element partition of the domain Ω and Γ_h the set of all the interior faces between the elements $\mathcal{T}_h$. Let $\Gamma_c \subset \Gamma_h$ be the subset of all faces where the displacement field is continuous and $\Gamma_f \subset \Gamma_h$ be the subset of facet that represent fractures.

The weak formulation of the elastic wave equation for the interior penalty discontinuous Galerkin method in fractured media is given by

$$\sum_{K\in\mathcal{T}_h}\int_K(\sigma(u),\varepsilon(v))dx - \sum_{K\in\mathcal{T}_h}\int_K \rho\omega^2 uvdx + \sum_{E\in\Gamma_b}\int_E i\rho\omega Auvds$$
$$- \sum_{E\in\Gamma_c}\int_E \{\tau(u)\}[v]\,ds - \sum_{E\in\Gamma_c}\int_E \{\tau(v)\}[u]\,ds + i\sum_{E\in\Gamma_c}\frac{\overline{\omega}}{h}\int_E(\lambda+2\mu)[u][v]\,ds$$
$$+ \sum_{E\in\Gamma_f}\int_E Z^{-1}[u][v]\,ds = \sum_{K\in\mathcal{T}_h}\int_K fvdx,$$

where $\overline{\omega}$ is the penalty parameter, $\tau(u) = \sigma(u)n$ is the traction vector, Γ_b is a subset of faces on the boundary. Here

$$u = Re(u) + iIm(u),$$

and $u = \sum_j u_j\phi_j$, ϕ_j are linear basis functions for the fine scale approximation.

We can write the complex valued problem of 2.1 in matrix form

$$(K_h + B_h - \omega^2 M_h)U = F_h, \tag{2.1}$$

where $U = Re(U) + iIm(U)$.

3 Multiscale Method

In this section, we describe construction of the multiscale basis functions and coarse grid approximation [9–14]. In the GMsFEM, we have following computational algorithm: (i) the construction of the multiscale basis functions by the solution of the local eigenvalue problem in local domain K and (ii) the construction and solution of the coarse grid approximation on multiscale space.

We define coarse grid $\mathcal{T}_H$ in domain Ω, $\mathcal{T}_H = \cup_{i=1}^{N_c} K_i$ with mesh sizes $H \gg h > 0$ where K_i is coarse cell (local domain), N_c is number of coarse cells. Let V_H be a finite dimensional function space, which consists of functions that are smooth on each local domain related to the coarse mesh cell. We construct two local multiscale spaces $V_H^K = V_H^{K,b} + V_H^{K,i}$ (boundary and interior) by solution

of the local eigenvalue problems on each coarse grid cell $K \in \mathcal{T}_H$. Furthermore, eigenfunctions corresponding to the dominant eigenvalues are used as the final multiscale basis functions. The resulting space is called the multiscale (offline) space for the coarse-grid block K. The global multiscale space V_H is then defined as the linear span of all these V_H^K, $K \in \mathcal{T}_H$ and will be used as the approximation space of IPDG coupling, which can be formulated as follows: find $u_H \in V_H$:

$$a_{DG}(u_H, v) - \omega^2 m(u_H, v) + ib(u_H, v) = l(v), \quad v \in V_H \tag{3.1}$$

where

$$a_{DG}(u,v) = \sum_{K\in\mathcal{T}_H} \int_K (\sigma(u), \varepsilon(v))dx - \sum_{E\in\Gamma_c} \int_E \{\tau(u)\}[v]\,ds - \sum_{E\in\Gamma_c} \int_E \{\tau(v)\}[u]\,ds$$
$$+ i \sum_{E\in\Gamma_c} \frac{\overline{\omega}}{h} \int_E (\lambda + 2\mu)[u][v]\,ds + \sum_{E\in\Gamma_f} \int_E Z^{-1}[u][v]\,ds,$$

$$m(u,v) = \sum_{K\in\mathcal{T}_H} \int_K \rho uv dx, \quad b(u,v) = \sum_{E\in\Gamma_b} \int_E \rho\omega Auv ds$$

$$l(v) = \sum_{K\in\mathcal{T}_H} \int_K fv dx$$

and $u = Re(u) + iIm(u)$.

For the construction of the boundary space, we solve following spectral problem in K

$$a_{DG}(\phi^{K,b}, v) = \lambda^b s(\phi^{K,b}, v), \quad v \in V_h(K), \tag{3.2}$$

where

$$s(\phi^{K,b}, v) = \int_{\partial K} \rho \phi^{K,b} v ds$$

To construct a multiscale space $V_H^{K,b}$, we select the first M^b eigenvectors $\phi_1^{K,b}$, $\phi_2^{K,b}$, ... , $\phi_{M^b}^{K,b}$ corresponding to the first M^b smallest eigenvalues $\lambda_1^b \le \lambda_2^b \le ... \le \lambda_{M^b}^b$, and define the space $V_b^{K,H}$ by

$$V_H^{K,b} = \text{span}\left\{\phi_1^{K,b}, \phi_2^{K,b}, ..., \phi_{M^b}^{K,b}\right\}. \tag{3.3}$$

Interior space $V_H^{K,i}$ is defined to capture interior eigenmodes for K and use following spectral problem with homogeneous Dirichlet boundary conditions to identify the important modes

$$\begin{aligned} a_{DG}(\phi^{K,i}, v) &= \lambda^i s(\phi^{K,i}, v), \quad v \in V_h(K), \\ \phi^i &= 0, \quad x \in \partial K. \end{aligned} \tag{3.4}$$

We select the first M^i eigenvectors $\phi_1^{K,i}, \phi_2^{K,i}, ..., \phi_{M^i}^{K,i}$ corresponding to the first M^i smallest eigenvalues $\lambda_1^i \le \lambda_2^i \le ... \le \lambda_{M^i}^i$. The space $V_H^{K,i}$ is spanned by the functions

$$V_H^{K,i} = \text{span}\left\{\phi_1^{K,i}, \phi_2^{K,i}, ..., \phi_{M^i}^{K,i}\right\}. \tag{3.5}$$

The coarse-scale system can be calculated by projecting the fine-scale matrices onto the coarse grid with the global projection matrix assembled from the calculated multiscale basis functions

$$R = (R_1, R_2, ..., R_N)^T, \quad R_j = \left[\phi_1^{K,i}, \phi_2^{K,i}, ..., \phi_{M^i}^{K,i}, \phi_1^{K,b}, \phi_2^{K,b}, ..., \phi_{M^b}^{K,b}\right]. \quad (3.6)$$

where R_j is the local projection matrix in a coarse element K_j and N is the number of coarse grid elements. In the numerical implementation, we first assemble the global matrices M_h, K_h, and vector F_h in (2.1). Then using the global projection matrix R, we can define the coarse-scale system

$$(K_H + B_H - \omega^2 M_H)V_H = F_H, \quad (3.7)$$

where $V_H = Re(V_H) + iIm(V_H)$, M_H and K_H are the coarse-scale mass stiffness matrices and B_H is the coarse-scale boundary mass matrix

$$M_H = RM_hR^T, \quad K_H = RK_hR^T, \quad B_H = RB_hR^T, \quad F_H = RF_h. \quad (3.8)$$

After calculation of the coarse-scale solution, we can recover the fine-scale solution, $V_{ms} = R^T V_H$.

4 Numerical Results

We present the results for the fine-scale solution and the coarse-scale solution using GMsDGM. The basis functions of the offline space are constructed by the procedure described above. For numerical simulations, we use the following parameters. Computational domains with different length of fracture are presented in Fig. 1 and have dimensions $\Omega = [0, L_x] \times [0, L_y]$ with $L_x = L_y = 500$[m]. On the left of Fig. 1, we have a fracture length of 10[m] (Case 1), and on the right of Fig. 1, we have a fracture length of 20[m] (Case 2). In all cases, we consider the fracture orientations to be the same.

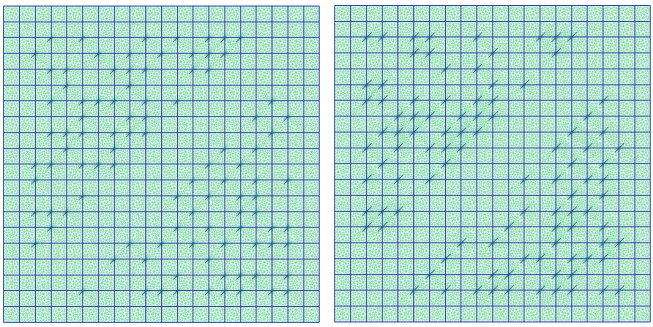

Fig. 1. Computational grids with different length of fractures (10[m] and 20[m]). Left: Case 1. Right: Case 2.

We set the source term $f(x) = G(x)P(\theta)$, where $P(\theta) = (cos\theta, sin\theta)$ is the polar angle of the source force vector with $\theta = 0$ and the spatial function $G(x)$ is defined as point source, $G(x) = \delta(x - x_0)$ with $x_0 = (250, 250)$ assigned as the center of the computational domain. We take penalty parameters $\varpi = 4$ and run simulations for $\omega = 2\pi f_0$ with $f_0 = 15$.
For numerical simulation, we set following parameters

$$K = \frac{E}{3(1-2\nu)}, \quad \mu = \frac{E}{2(1+\nu)}, \tag{4.1}$$

with $E = 40 \cdot 10^9$[Pa], $\nu = 0.3$, $\rho = 2300[kg/m^3]$. For fracture compliance matrix Z in (1.3), we use $z_1 = z_2 = 10^7$[m/Pa].

For the numerical solution, we construct structured coarse grids with 400 cells. The fine grids are unstructured grids that resolve the fractures.

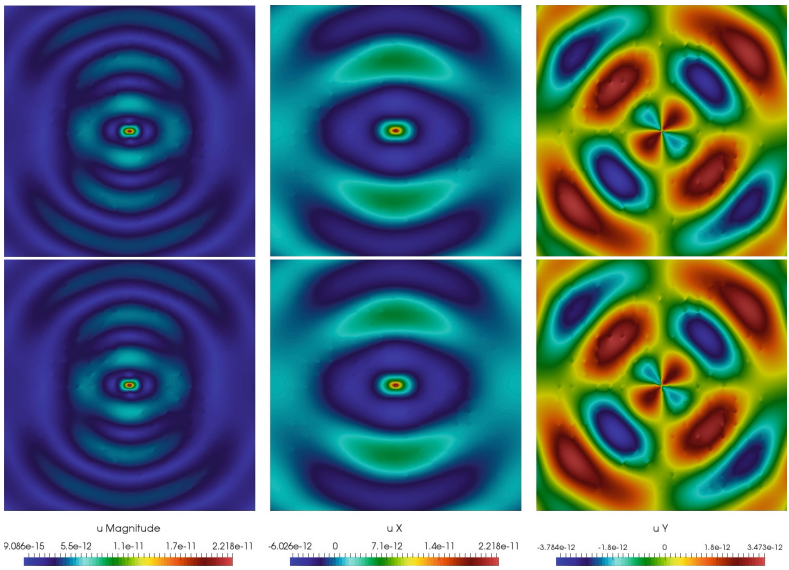

Fig. 2. Fine-scale (top) and coarse-scale (bottom) solution for magnitude, X and Y (from left to right) for Case 1.

For the Case 1, fine grid contains 16077 vertices and 31752 triangle elements. Fine grid for Case 2 contains 16509 vertices and 32616 triangle elements (see Fig. 1). Coarse grid contains 441 vertices and 400 rectangular elements are the same for Case 1 and Case 2.

In Fig. 2, we present fine-scale and multiscale solutions for Case 1. Calculations was performed using 25 boundary and 25 interior multiscale basis functions. Size of coarse grid system is $DOF = 40000$. In Fig. 3, we present fine-scale and multiscale solutions for Case 2. Calculations was performed in the same way as

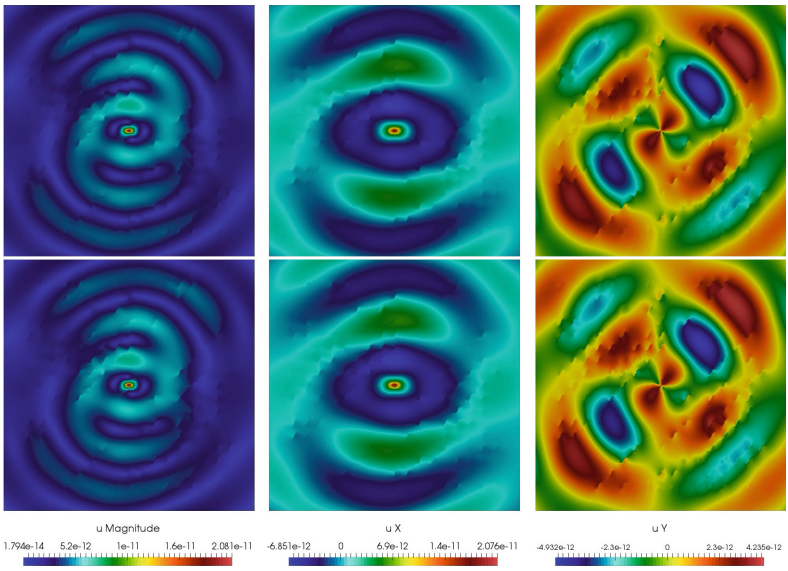

Fig. 3. Fine-scale (top) and coarse-scale (bottom) solution for magnitude, X and Y (from left to right) for Case 2.

Table 1. Relative errors for different number of multiscale basis. Case 1

$M_i + M_b$	L_2 (%)	$M_i = 0, M_b$	L_2 (%)
5+ 5	92.4309	5	92.0936
10+10	20.0548	10	22.5863
15+15	7.58553	15	10.1345
20+20	4.06103	20	5.94387
25+25	3.48032	25	4.15289

Table 2. Relative errors for different number of multiscale basis. Case 2

$M_i + M_b$	L_2 (%)	$M_i = 0, M_b$	L_2 (%)
5+ 5	98.481	5	98.4668
10+10	26.5191	10	26.7304
15+15	9.20703	15	8.55055
20+20	7.42222	20	8.68984
25+25	6.32786	25	9.39684

in Case 1 using 25 boundary and 25 interior multiscale basis functions. Size of coarse grid system is $DOF = 40000$. We obtain good solution for reduced order model using GMsDGM.

Relative L_2 errors are shown in Table 1 and 2, where M_i and M_b are the numbers of the multiscale interior and boundary basis functions. When we have zero interior bases $M_i = 0$ (in Table 1 and 2, right table) the errors increase. From the both tables we observe that the interior multiscale basis functions can reduce errors.

We present numerical results for two geometries with different size of fractures (10 m and 20 m). We construct reduced order model using Generalized Multiscale Discontinuous Galerkin Finite Element Method. Our results show that the presented method give good approximation of the solution and reduce size of system.

Acknowledgments. Work is supported by the mega-grant of the Russian Federation Government (N 14.Y26.31.0013).

References

1. De Basabe, J.D., Sen, M.K., Wheeler, M.F.: Seismic wave propagation in fractured media: a discontinuous Galerkin approach, SEG Expanded Abstr 30 (2011)
2. De Basabe, J.D., Sen, M.K., Wheeler, M.F.: Elastic wave propagation in fractured media using the discontinuous Galerkin method. Geophysics **81**(4), T163–T174 (2016)
3. Zhang, J.: Elastic wave modeling in fractured media with an explicit approach. Geophysics **70**(5), T75–T85 (2005)
4. Schoenberg, M.: Elastic wave behavior across linear slip interfaces. J. Acoust. Soc. Am. **68**(5), 1516–1521 (1980)
5. Engquist, B., Majda, A.: Absorbing boundary conditions for numerical simulation of waves. Proc. Nat. Acad. Sci. **74**(5), 1765–1766 (1977)
6. Grote, M.J., Schneebeli, A., Schötzau, D.: Discontinuous Galerkin finite element method for the wave equation. SIAM J. Numer. Anal. **44**(6), 2408–2430 (2006)
7. Arnold, D.N.: An interior penalty finite element method with discontinuous elements. SIAM J. Numer. Anal. **19**(4), 742–760 (1982)
8. Lahivaara, T.: Discontinuous Galerkin Method for Time-Domain Wave Problems. University of Eastern Finland, Joensuu (2010)
9. Efendiev, Y., Galvis, J., Hou, T.Y.: Generalized multiscale finite element methods (GMsFEM). J. Comput. Phys. **215**, 116–135 (2013)
10. Chung, E.T., Efendiev, Y., Leung, W.T.: An online generalized multiscale discontinuous Galerkin method (GMsDGM) for flows in heterogeneous media. Commun. Comput. Phys. **21**(2), 401–422 (2017)
11. Chung, E.T., Efendiev, Y., Leung, W.T.: Generalized multiscale finite element methods for wave propagation in heterogeneous media. Multiscale Model. Simul. **12**(4), 1641–1721 (2014)
12. Gao, K., Fu, S., Gibson, R.L., Chung, E.T., Efendiev, Y.: Generalized multiscale finite-element method (GMsFEM) for elastic wave propagation in heterogeneous, anisotropic media. J. Comput. Phys. **295**, 161–188 (2015)
13. Chung, E.T., Efendiev, Y., Gibson, R.L., Vasilyeva, M.: A generalized multiscale finite element method for elastic wave propagation in fractured media. GEM-Int. J. Geomath. **7**(2), 163–182 (2016)
14. Chung, E.T., Efendiev, Y., Fu, S.: Generalized multiscale finite element method for elasticity equations. GEM-Int. J. Geomath. **5**(2), 225–251 (2014)